An integrated data-driven methodology for early fault detection and diagnosis in nuclear power plant

WANG Hang[1], PENG Minjun[1], WANG Gang[1], LI Wei[1], LIU Yongkuo[1], CHENG Shouyu[1], and AYODEJI Abiodun[1, 2]

1. Key Subject Laboratory of Nuclear Safety and Simulation Technology, Harbin Engineering University, Harbin, Heilongjiang, 150001, China (wanghang1990312@126.com)

2. Nuclear Power Plant Development Directorate, Nigeria Atomic Energy Commission, Abuja, Nigeria (1158435404@qq.com)

Abstract: In a nuclear power plant, severe accident may result from unchecked malfunctions and human error, and it could lead to radiological release to the immediate surroundings and global ecological environment. However, a reliable fault detection and diagnosis methodology could inform the operators about the current situation of the plant and assist them to locate and diagnose the malfunction accurately and properly. This paper presents an integrated data-driven methodology for an on-line fault diagnosis in a nuclear power plant. One of the merits in this methodology is that it utilizes all the plant measured parameters to perform on-line training and simultaneously implement diagnostic task. In addition, the related algorithms in different phases of the diagnostic system are optimized to avoid incorrect results and reduce false alarms. The proposed method utilizes improved principle component analysis model to detect abnormalities. Furthermore, on-line artificial immunity algorithm is adopted to recognize the fault type based on the already existing simulation model. Consequently, some typical distance formulae for similarity measurement – the Euclidean distance and the Mahalanobis distance - are applied for on-line failure degree evaluation. The performance of this methodology is verified by applying it to the Reactor Coolant System of a Pressurized Water Reactor. The results show that this improved data-driven methodology utilized for fault detection and diagnosis is feasible and practical. More significantly, it is handy to enhance the research depth on computerized operator support system and on-line risk monitoring, which will assist operators to make decision and operation.

Keyword: fault diagnosis; principle component analysis; artificial immunity algorithm; similarity measurement; pressurized water reactor

1 Introduction

A nuclear power plant contains hundreds of sub-systems and numerous monitoring and control parameters, and a significant number of these systems are mutually coupled with each other [1]. The complexity in these couplings is especially noticeable when malfunctions in a power plant occur. Although reactor operators have gone through numerous trainings over time, in certain situations it's still difficult for them to accurately assess the fault in a very short period of time [2]. This is mainly as a result of the huge psychological pressure the operators always face when fault occurs. Also, a large number of scattered alarms may delay or even disturb the operator judgement to carry out effective identification and operation, which ultimately lead to human errors with serious effect on the safety of nuclear power plants [3]. It could then lead to radiological release to the immediate surroundings and global ecological environment [4].

Therefore, it's necessary to study effective fault detection and diagnosis methods for nuclear power plants. That is methods with capability to extract the major symptoms and information to assist the operators to make accurate judgments and decisions [5], so as to effectively prevent incipient faults from resulting in a severe accident. As for the economy of nuclear power plants, early and timely fault diagnosis can reduce unscheduled maintenance tasks and unnecessary shutdown of reactor [6]. Meanwhile, with the development of digital instrument control system (I&Cs), the third-generation nuclear power technologies such as AP1000, EPR, *etc*. are widely utilizing digital I&Cs which could provide more information and parameters than the traditional one [7]. Thus, it is more convenient for the design and development of data-driven fault diagnosis methodologies. More importantly, the fault diagnosis

Received date: June 1, 2017
(Revised date: July 13, 2017)

method can conversely improve the intelligent and information level of digital I&Cs to ensure the safe operation of the nuclear power plant [8]. At the same time, from the current-development-trend perspective, small modular reactors may be utilized in special areas for energy supply such as in remote islands, offshore drilling platforms and even international space stations such as the "isolated island", with very few operating crew. Hence, the prospective application of modular reactors requires an urgent need for intelligent detection and fault diagnosis technology.

Researchers all over the world have done a lot of research on anomaly detection and fault diagnosis, and these researches can be divided into two categories: One is based on qualitative knowledge such as expert systems, graph theory, qualitative mathematical models, fuzzy logic, *etc* [9]. The diagnostic system developed by Europe Halden project can identify typical faults for system and device based on knowledge of experts [10]. The PRODIAG diagnostic system developed by the Argonne National Laboratory can utilize function-based and component-based features for qualitative fault diagnosis [11]. However, the acquisition of knowledge is the difficulty in these methods, because nuclear power plants are complex nonlinear systems, and there may be shortcomings such as rule matching conflict and combinatorial explosion in qualitative reasoning process. In addition, the knowledge-based system, like most diagnostic systems, can sometimes provide incorrect diagnostic results.

Another diagnostic method is the data-driven approach, mainly divided into statistical methods and non-statistical methods [12]. The statistical methods primarily contain PCA, partial least squares, and their variants, and they have been successfully implemented in a number of systems. The University of Tennessee utilizes the PCA algorithm to identify system failures and model uncertainties [13]. China Atomic Energy Institute uses PCA algorithm to diagnose the faults in main coolant pumps. Other non-statistical methods mainly include artificial neural network, support vector machine, Bayesian network, and artificial immune algorithm. Using the fuzzy neural network, Zio studied the fault diagnosis method of CANDU-6 nuclear reactor main coolant pump [14]. Wolbrecht applied Bayesian network model to diagnose the power failure of the equipment, confirming the suitability of the model in engineering applications [15]. Ishiguro adopted the immune network model for on-line fault diagnosis of equipment [16]. However, the major drawback of these methods is the over-reliance on historical data, which is often difficult to obtain. At the same time, the unexplainable diagnostic results could not convince the operators.

In summary, qualitative knowledge-based methods have some limitations in knowledge acquisition and qualitative reasoning; the data-driven method requires a large number of historical data under failure scenario, and the actual failure data cannot be created artificially in nuclear power plant. Moreover, utilizing corresponding experimental equipment for data acquisition is not economical. Thus, most of the current fault diagnosis methods utilize full-scope simulator to not only simulate the actual NPP, but also experiment with a variety of failure scenario. Hence, the results of abnormality detection and fault diagnosis are too idealistic because of the problems with acquiring data that represent fault situations. With the development of simulation technology, it is possible to establish a mechanism simulation model which could run synchronously with NPP by acquiring real-time process parameters through I&Cs. When a failure occurs, thermal-hydraulic mechanism simulation model is switched from on-line operation to off-line faster-than-real-time status to quickly calculate the change trends [17]. These simulation data obtained from simulation model could reflect the current status of NPP after failures, which will not only solve the problem of sample data acquisition, but also eliminate the uncertainty caused by different configurations.

Based on the existing on-line simulation model, this paper studies the improved PCA-based algorithm. Artificial immunity algorithm (AIA) and some typical distance functions in similarity measurement are combined in the system-level on-line fault detection and diagnosis methodology. Compared with the traditional data-driven methods, fault detection based on PCA is combined with false alarm reducing algorithm based on binomial distribution which is

more practical in engineering application. In addition, AIA and two typical distance functions could do on-line learning and training with all measurements for fault type diagnosis and degree assessment. Inevitably, the thermal-hydraulic mechanism simulation model have a certain calculation errors compared with the actual operating parameters. However, the integrated data-driven method described in this paper has a strong fault tolerance capability which can extract the main features of abnormal parameters to perform fault diagnosis. Hence, the hybrid approach serves as a form of make up for the on-line simulation model to improve the practicability and accuracy of data-driven fault diagnosis.

The methodology presented in this paper has a wide scope of application in Pressurized Water Reactor (PWR) systems, and by extension, any other types of NPP. This paper considers the Reactor Coolant System (RCS) of a PWR as research case study to discuss and examine the integrated data-driven methodology and to evaluate its performance. The paper is organized as follows. Section 2 provides a description of the theoretical background of the approach utilized for fault detection, fault diagnosis. The assessments of the fault detection and false alarm reducing method based on PCA is presented in Section 2.1; the fault diagnosis methods using AIA is discussed in Section 2.2; The process of combining the PCA and similarity measurement for failure degree evaluation are discussed in Section 2.3. Section 3 presents the constitution and development of hybrid fault detection and diagnosis methodology. Section 4 describes the test results of simulation experiments. Finally, the concluding remarks are summarized in Section 5.

2 Theory and methodology of fault detection and diagnosis

2.1 Overview

The purpose of integrating several data-driven approaches is to take advantage of their individual merits and to compensate for their defects. This step is believed to further enhance the accuracy and effectiveness of fault diagnosis. In this work, the PCA model and binomial probability distribution are integrated to detect the abnormalities as quickly as possible and reduce false alarm to the minimum. Moreover, the AIA inspired by the biological immunity phenomenon is applied for fault type diagnosis. AIA for fault diagnosis shows great advantages in on-line training and gives accurate pattern recognition. After locating the fault type, the failure magnitude should be evaluated for typical faults which is significant for operators to evaluate the current status of the NPP. As parameters under different failure degrees are totally different from each other, PCA and some distance functions for similarity measurement are combined to achieve the assessment of failure degree. Specifically, the framework of the diagnostic system is as shown in Fig.1, and its processes are as described below:

Step 1: The plant measurements are acquired real-time from I&Cs and stored into a database, according to the layout of sensors.

Step 2: An optimized PCA-based model is utilized to detect the faults by analyzing the real-time data. After detecting the abnormalities, the on-line mechanism simulation model is transferred to the off-line calculation to provide training data for AIA and similarity measurement.

Step 3: During the diagnostic process, AIA adopts different simulated data as training data and matches the output with the real-time data at the same time to get the results.

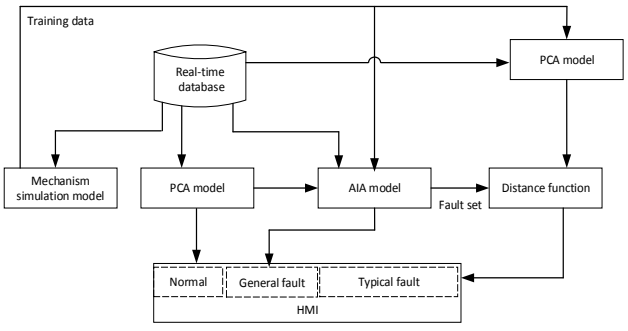

Fig.1 Framework of the integrated data-driven methodology

Step 4: If the malfunction is a general fault (wrongly-opened or wrongly-closed pumps and valves) the results will be displayed in the human machine interface (HMI). However, if the malfunction is a gradual fault such as a small leakage in the pipeline, containers or heat exchangers, the failure magnitude will be assessed.

Step 5: Then the PCA model is used for reduction of data dimension to acquire the major features of real-time and simulated data, and the Euclidean and the Mahalanobis distance models are utilized to evaluate the corresponding degree of the fault. Further, the results from these distance models are compared and analyzed, leading to a decision on their suitability for the task. Finally, the entire information on the malfunction will be shown in HMI.

2.2 Fault detection based on enhanced PCA model

PCA-based method is one of the multivariate statistical techniques, and it utilizes orthogonal transformation to convert the high-dimensional multivariate information into low dimensional information. Thus, it has obvious advantage in feature extraction and data compression [18].

For traditional threshold-based fault detection, numerous parameters are selected to obtain enough information, but too many parameters will increase the difficulty of detecting the abnormalities. Hence, PCA model calculate the statistics in principal space and residual error space, which is much more sensitive than threshold-based method. This approach proves to be more accurate and faster for abnormality detection.

The PCA-based abnormality detection is mainly used for the linear process; hence it could work efficiently for a linear system. However, a nuclear reactor is a typical non-linear system. If PCA model is directly utilized for on-line monitoring in a non-linear system, there may be numerous false alarms which will have a strong impact on the normal operation of NPP. Hence, the false alarm reducing PCA algorithm based on binomial probability distribution is adopted. The framework of fault detection and false alarm reduction is shown in Fig.2:

The array $X_{n\times m}$ is the new data matrix, where n means the dimension of samples and m means the number of samples. According to the theory of PCA, after normalization and standardization of these data, the covariance matrix of $X_{n\times m}$ is:

$$C_x = P_{m\times m} D_\lambda P^T_{m\times m} \tag{1}$$

Where, D_λ is the eigenvalue matrix shown as $diag(\lambda_1, \lambda_2, \cdots, \lambda_m)$, and P is the eigenvector matrix of $X_{n\times m}$.

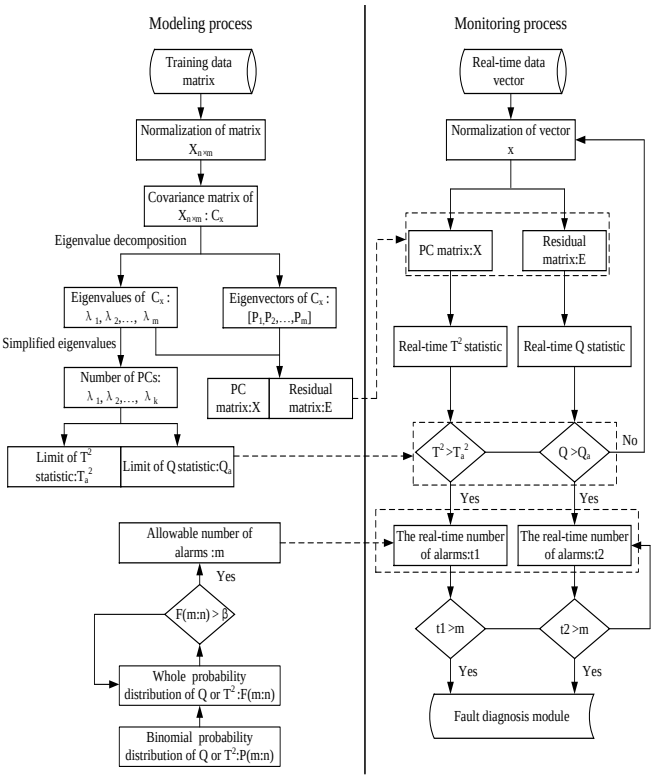

Fig.2 The framework of fault detection and false alarm reduction

Furthermore, the number of PCs is determined based on the eigenvalues. In this paper, a cumulative percent variance (CPV) is adopted, from which the variation in PCs could approximately represent the variation of the selected PCs:

$$CPV = \frac{\sum_{i=1}^{i=l} \lambda_i}{\sum_{i=1}^{i=m} \lambda_i} \times 100\% \tag{2}$$

Where, l < m is the number of PCs. For the selected PCs, the original data matrix X can be decomposed into a PC matrix $\hat{X}$ which contains the information on system variation, and a residual matrix E which contains information on noise or model error. Consequently, the matrix X is represented as:

$$X = \hat{X} + E \tag{3}$$

Where, $\hat{X}$ is the ideal values of X, and E signifies the errors in the model. $\hat{X}$ and E are represented by PCA as follows:

$$\hat{X} = \hat{T}\hat{P}^T = X_{n\times m}\hat{P}_{m\times l}\hat{P}^T_{m\times l} \quad (4)$$

$$E = \tilde{T}\tilde{P}^T = X_{n\times m}\tilde{P}_{m\times(m-l)}\tilde{P}^T_{m\times(m-l)} \quad (5)$$

Where $\hat{T}$ and $\tilde{T}$ are the score vector which represent the principal components (PCs) and $\hat{P}$ and $\tilde{P}$ mean the load vector.

As shown in Fig. 2, during the detection process, Q statistic which measures the variance in residual space E and Hotelling's T^2 statistic that represents the variance in PC space $\hat{X}$ are calculated for a real-time vector $x = [x_1, x_2, ..., x_m]$ as:

$$Q = x\left(I - P_l P_l^T\right)x^T \le Q_a \quad (6)$$

$$T^2 = t_i D_\lambda^{-1} t_i^T = x P_l D_\lambda^{-1} P_l^T x^T \le T_a^2 \quad (7)$$

Where, Q_a and T_a^2 derived from training process are the statistic limit for Q and T^2 statistics, respectively [19], and I is the unit matrix. If the Q or T^2 statistics exceed the corresponding limits, alarm will be triggered and fault diagnosis module will be activated.

As false alarms may occur due to the fact that NPP is a non-liner system and coupled with auto-control logics, it is essential to reduce the events of false alarms to the bearest minimum. In this paper, binomial distribution is combined to achieve this aim. We suppose that the false alarm probability of Q and T^2 statistics is μ for every second and all real-time data are independent of each other, so the probability distribution of T^2 or Q statistics is represented as:

$$P(a:b) = C_b^a u^a (1-u)^{b-a} \quad (8)$$

Where, "b" is set as the observation window and "a" is the frequency of false alarms in observation window. Then the whole probability in "a" seconds is:

$$F(a:b) = \sum_{i=0}^{a} C_b^a u^a (1-u)^{b-a} < \beta \quad (9)$$

Further, a false alarm tolerance β is utilized to restrict the largest allowable m derived from Formula 9. β is an experience value according to the statistical experience in the monitoring process.

Thus, during the monitoring process, the real-time data vector will be tested by the PC matrix and residual matrix to get the real-time T^2 and Q statistics. If the T^2 and Q statistics exceed the limits at any time, then further T^2 and Q statistics will be analyzed in the observation window b. For real-time data, if the number of alarms is more than the calculated number m, then a true abnormality is detected and alarms will be triggered. Considering the sensitivity of fault detection, a large value for the length of observation window is unacceptable for delaying the time for diagnosis and analysis. However, a very small value is also improper. As a result, in this paper b=8 is adopted for the length of observation window.

2.3 On-line fault type diagnosis utilizing AIA

AIA is derived from the study of biological immune system. By imitating the body's immune system, antigen-antibody recognition, self-adjusting, cell differentiation and other functions are realized [20]. In addition, antigen-antibody identification is one of the significant functions in biological immune system which attracts the attention of diagnostic researchers and it is being applied for pattern recognition problems [21]. The merits of this method are self-organization, distributed parallel processing, self-taught learning, noise tolerance and good robustness providing a new thought for pattern recognition and fault diagnosis [22].

As one of the data-driven methods developed in recent years, AIAs are similar with artificial neural network (ANN) in their requirements for numerous sample data under normal and different failure situations for network training and learning. However, this demerit could be avoided when combined with mechanism simulation model with capability to calculate parameter values faster-than-real-time to provide sample data under different failure modes. The following are the merits of AIA compared with ANN:

(1) For ANN, weights and thresholds are utilized to represent the relation between inputs and outputs. But, an accurate ANN needs multi-layer network structure which may lead to inferior on-line learning ability and long time for training. Conversely, AIA utilizes antigen and other antibodies to train network which requires much less time for on-line training and learning.

(2) If too many inputs are selected with ANN for on-line fault diagnosis, the network structure will

become complex, which further influences the convergence of network. Therefore, some of the measurements are used as inputs of ANN, although there will be greater uncertainty which may omit parts of the available information. On the contrary, the proposed AIA model do not need to select parameters, it utilizes all the measurements for fault diagnosis which will obviously reduce uncertainties because of the selected input parameters.

The proposed algorithm is one of the branches in AIA, which is based on the theory presented by Tarakanov [23], which asserts that the lowest binding energy is generated by antigen and antihelion which belongs to its own cell tissue. Figure 3 displays the framework for diagnosing fault type:

(1) During the on-line training processes, simulated data under normal and different failure modes are acquired from simulation model, named as $X_{normal}=(x_{i1},x_{i2},...,x_{in})$, $X_1=(x_{i1},x_{i2},...,x_{in})$, $X_2=(x_{i1},x_{i2},...,x_{in})$, $X_m=(x_{i1},x_{i2},...,x_{in})$. Where, m represents the number of fault types, n means the number of measurements and i expresses the time series of data. Further, they are normalized and standardized to eliminate the influence of dimension.

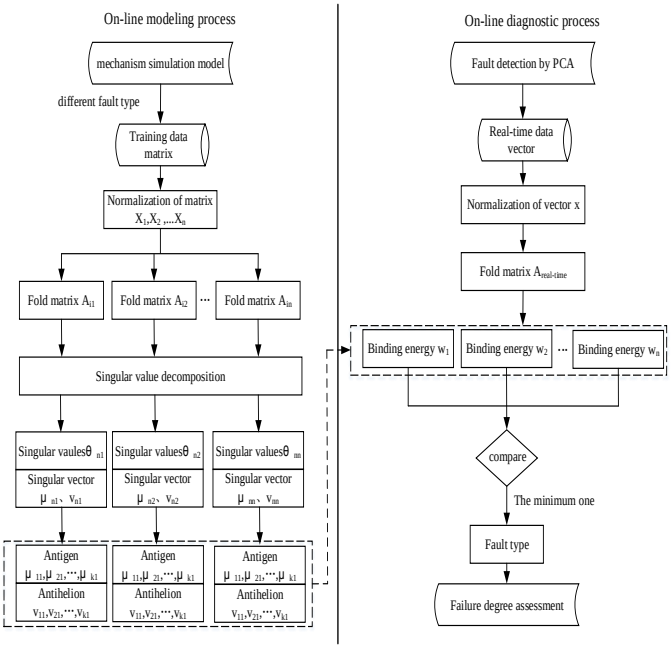

Fig.3 Flow chart of fault type diagnosis based on AIA

(2) X_{normal}, X_1, X_2 …, X_n in every second are folded into data matrix, and named as A_{normal}, A_{i1}, A_{i2},…, A_{in}.

(3) In order to get antigen and antihelion, the data matrix is utilized to do singular decomposition in every second. For $A\in C^{m\times n}$, there is orthogonal matrix

$U=[u_1,u_2,u_3,\cdots,u_m]\subset C^{m\times m}$,

$V=[v_1,v_2,v_3,\cdots,v_n]\subset C^{n\times n}$:

$$A=U\begin{bmatrix}\Delta & 0\\ 0 & 0\end{bmatrix}V^H=\theta_1u_1v_1^T+\theta_2u_2v_2^T+\theta_3u_3v_3^T+\cdots+\theta_ru_rv_r^Tz \quad (10)$$

Where, $\Delta=diag(\theta_1,\theta_2,\theta_3,\cdots,\theta_r)$, and θ_i is the singular value of matrix A. u_i is the left singular vector and v_i is right singular vector. In addition, r is the sequence of matrix A. As u_i , v_i are vectors, $u_iu_i^T=0$, $v_iv_i^T=0$, $i=1,2,3,\cdots,r$.

According to the character of singular decomposition: for each singular value, $\theta_1\geq\theta_2\geq\theta_3\geq\cdots\geq\theta_n\geq 0$. Also, singular value represents significant information and according to the theory of matrices the bigger the singular value is, the more important it will be. In order to utilize simple data matrix to replace complex matrix, the number of singular values are as shown below:

$$(\theta_1+\theta_2+...+\theta_k)/\sum_1^n\theta_i\geq 90\% \quad (11)$$

where, k is the selected number of singular values, and n represents the total number of singular values。 Therefore, matrix A could be simplified as：

$$A\approx\theta_1u_1v_1^T+\theta_2u_2v_2^T+...+\theta_ku_kv_k^T \quad (12)$$

(4) After selecting antigen and corresponding antihelion for every second under different failure modes, the real-time data matrix will be normalized, folded and combined with these antigen and antihelion respectively to perform on-line fault diagnosis. As the binding energy will be lowest while the real-time data matrix is combined with antigen and corresponding antihelion of the same failure mode, the exact fault will be diagnosed. Specifically, u_i, v_i are considered as antigen and corresponding antihelion. Finally, the binding energy is shown as Eq. 13.

$$W_i=-(u_1^TAv_1+u_2^TAv_2+...+u_k^TAv_k) \quad (13)$$

where k is the selected number of antigen and antihelion.

2.4 Failure degree assessment by combining PCA and similarity measurement

After diagnosing the fault type, PCA and similarity measurement was carried out to assess the degree of the faults. Similarity measurement is a kind of machine learning methods, and has already been applied in the complex chemical process, power line fault detection, biological genetic testing and so on [24]. However, with respect to the aspect of fault magnitude evaluation, the method is relatively limited, and rarely applied to the analysis of NPP. Lang distance, Chebyshev distance and Ming distance are frequently used distance functions for similarity measurement. In this paper, we select two typical distance functions: Euclidean distance and Mahalabonis distance for failure degree evaluation respectively. Besides, the effectiveness of these different distance functions will be validated and compared.

Euclidean distance is the most common distance function in our daily life, it reflects the real distance of two points in the multi-dimensional space and utilizes the whole distance to calculate the similarity with each other. But there are obvious shortcomings because it will equally treat each parameter in the data matrix which may not meet the practical requirements. In an n-dimension, Euclidean distance is represented as follows:

$$d_{12}=\sqrt{\sum_{k=1}^{n}\left(x_{1k}-x_{2k}\right)^{2}} \qquad (14)$$

Where $\left(x_{11},x_{12},x_{13},\cdots,x_{1n}\right)$, $\left(x_{21},x_{22},x_{23},\cdots,x_{2n}\right)$ are two points in dimension n space, $k=1,2,3,\cdots,n$.

Mahalanobis distance is used to measure the covariance distance in different sample data [25]. It can efficiently calculate the gravity distance between a sample and its sample sets. Besides, it can also eliminate the correlation between variables and reflect the relationship between each feature. In comparison with Euclidean distance, Mahalanobis distance is not affected by dimension scaling. In fact, Mahalanobis distance also considers the relationship between various parameters in a more comprehensive and scientific manner. We suppose there is i parameters in data matrix X, and the average vector is $\mu=(\mu_1,\mu_2,\ldots,\mu_i)^T$, C_x is the corresponding covariance matrix of data matrix X. Therefore, the Mahalanobis distance of real-time vector and each data matrix is given by

$$d_2=\left(y-\mu\right)^T C_x^{-1}\left(y-\mu\right) \qquad (15)$$

During the evaluated process, parameters should be selected for distance function model. However, the selection of parameters may be greatly subjective. And we cannot always choose the parameters which will be applicable for the entire failure scenario. In order to solve this problem, PCA model is implemented to reduce data dimension and to choose fewer principle components for estimation of the original data [26], as shown in Fig. 4:

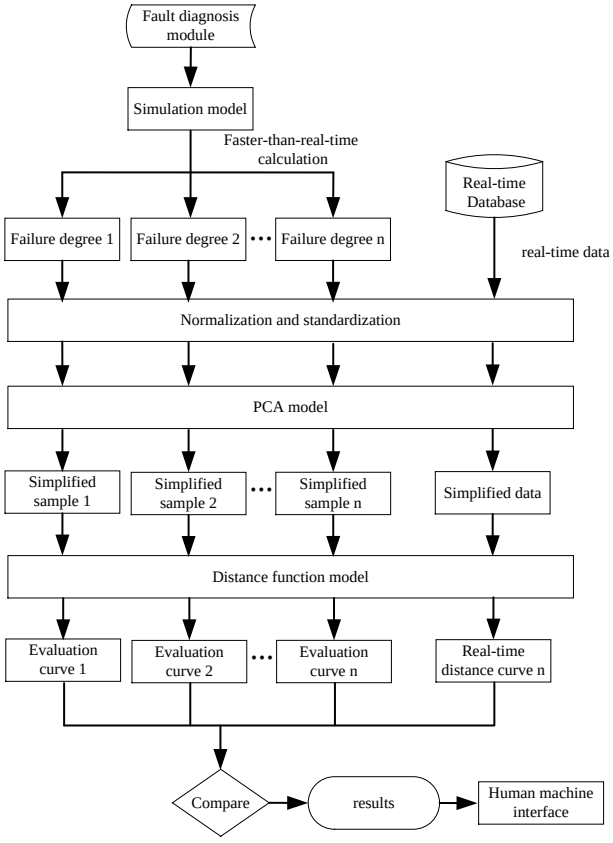

Fig.4 Flow chart of fault degree evaluation.

(1) After diagnosing the fault type with AIA, the sample data of this fault under different magnitudes are provided by simulation model.

(2) Real-time data and different simulated data are normalized and standardized together.

(3) According to the theory of PCA as defined in section 2.2, eigenvalue decomposition is done after getting the covariance matrix. Further, parameter estimation of the original matrix will be obtained after selecting the principal components.

(4) These simplified parameters are considered as $O_1(t)$ in m-dimensional space. In order to evaluate the current failure degree of RCS, polynomial fitting methods are adopted, where time is the independent variable and distances values D_{it} is the dependent variable. After computing curves for different failure degree， numerical integration of these curves, ΣD_{it} is done respectively.

(5) The real-time data are calculated through the same process as mentioned above so that numerical integration of real-time curve Σd_t will be obtained and compared with ΣD_{it}. Hence, the corresponding integrals value of ΣD_{it} that is closest to that of Σd_t is the failure degree i. However, if the difference between the integral value of ΣD_{it} and Σd_t is large, the nearest value of ΣD_{it} compared with Σd_t is stored. And then the simulation model will compute faster-than-real-time to provide more sample data around ΣD_{it} for Mahalanobis distance function until the results of failure degree are within the acceptable range.

3 Simulation test and results

3.1 Obtaining and selection of related parameters

It is pertinent to note that there are challenges with performing specific experiments on operating NPP to acquire real data with fault signatures. Consequently, the 300MW Qinshan NPP full scope simulator developed by Harbin Engineering University is utilized as a real NPP, and this paper assumes that the data collected is reliable. This NPP is a two-loop pressurized water reactor and the full thermal power is 966MW. The natural circulation steam generators (SG) are used to transfer the heat to the secondary side. In addition, the layout of the sensors in RCS of 300MW Qinshan NPP and the corresponding parameters' values under 100% reactor operating status are shown in Table 1. The table also contains the simulated values during steady operation, derived by utilizing thermal-hydraulic mechanism simulation model.

In this research work, the proposed data-driven methodology is developed by MATLAB and C# programming. General faults such as miss-operated pumps and valves can be easily detected and analyzed by digital I&Cs. Thus, in order to test the functionality of the proposed methodology, a 2 cm^2 leakage fault in 1# cold leg pipeline is inserted at random after 300s of steadily running the NPP simulator at 100% power. In the incipient nature of this fault, the trends of the parameters change slightly, and the safety injection system is not activated. Moreover, the coolant pumps and SGs are all in normal operating mode because of the compensation/remission from proportional heaters in the pressurizer and the charging flow from chemistry and volume control system. Thus, detecting and accurately diagnosing this fault by the operator is difficult. Hence, the integrated data-driven fault diagnosis system is beneficial for these kinds of faults. In Fig. 5, some measurements are displayed under normal and abnormal conditions.

Table1 layout of measurements in RCS

No.	Sensors	Measured values	Simulated values
1	1# outlet pressure of reactor vessel	15.428MPa	15.432MPa
2	2# outlet pressure of reactor vessel	15.428MPa	15.432MPa
3	1# outlet temperature of reactor vessel	588.54K	588.41K
4	2# outlet temperature of reactor vessel	588.54K	588.41K
5	Pressure of pressurizer	15.418Mpa	15.424Mpa
6	Water level of pressurizer	5.40m	5.41m
7	Temperature of steam in pressurizer	617.42K	617.52K
8	1# Outlet flow through SG to pump	3338.52kg/s	3338.13kg/s
9	2# Outlet flow through SG to pump	3338.72kg/s	3338.13kg/s
10	1# feed water flow of SG	260.12kg/s	259.57kg/s
11	2# feed water flow of SG	259.78kg/s	259.85kg/s
12	1# steam pressure of SG	5.518MPa	5.524MPa
13	2# steam pressure of SG	5.518Mpa	5.524Mpa
14	1# steam temperature of SG	543.36K	543.37K
15	2# steam temperature of SG	543.36K	543.37K
16	1# water level of SG	10.47m	10.47m
17	2# water level of SG	10.47m	10.47m
18	1# outlet steam flow	259.86kg/	259.84kg/s

	of SG	s	
19	2# outlet steam flow of SG	259.86kg/s	259.84kg/s
20	1# inlet pressure of reactor vessel	15.55MPa	15.58MPa
21	2# inlet pressure of reactor vessel	15.55MPa	15.58MPa
22	1# inlet flow of reactor vessel	3338.52kg/s	3338.13kg/s
23	2# inlet flow of reactor vessel	3338.52kg/s	3338.13kg/s
24	1# inlet temperature of reactor vessel	562.34℃	562.43℃
25	2# inlet temperature of reactor vessel	562.34℃	562.44℃
26	Water level of reactor vessel	9.53m	9.53m

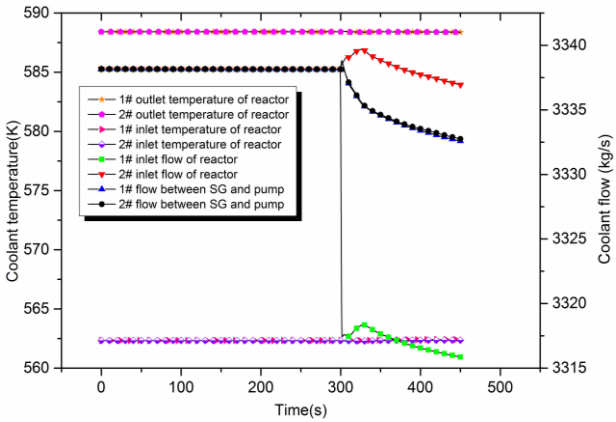

Fig. 5(a) Measurements under normal and abnormal conditions.

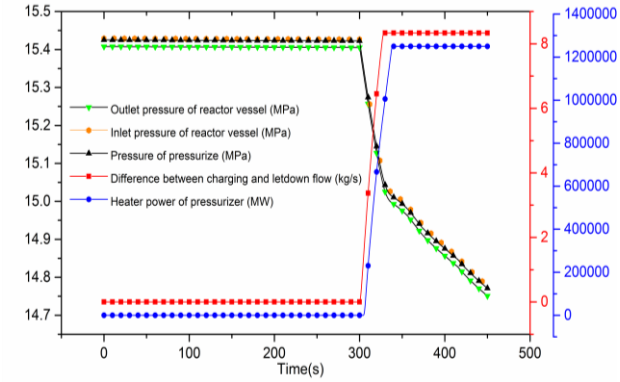

Fig. 5(b) Measurements under normal and abnormal conditions.

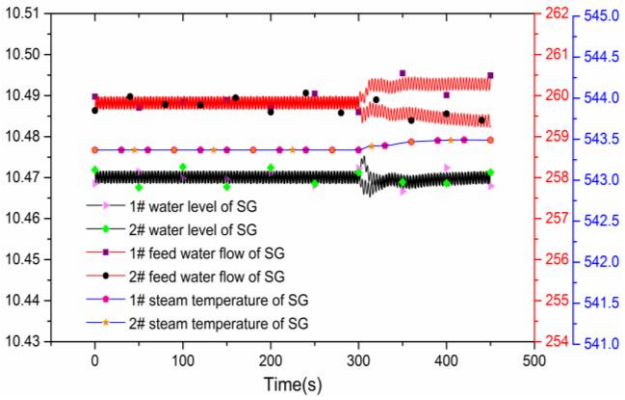

Fig. 5(c) Measurements under normal and abnormal conditions.

3.2 Rapid and accurate faults detection

As stated in section 2.2, we suppose that the false alarm probability of T^2 and Q statistics are μ for every second. According to the statistical experience as applied in nuclear industries, the commonly used experience value for μ is between 0.0 and 0.05. In addition, for a false alarm tolerance β, its common value is around 0.95 to 0.99. Therefore, the number of allowable false alarm m in time window n are shown in Table 2 under different values of μ and corresponding β. Consequently, considering the common situation, μ=0.05 and β=0.99 are selected for fault detection. Thus, the allowable false alarm is 3 in 8s time windows.

Table 2 allowable false alarm m in 8s time windows

	μ=0.01	μ=0.02	μ=0.03	μ=0.04	μ=0.05
β=0.99	2	3	3	3	3
β=0.97	2	2	3	3	3
β=0.95	2	2	2	2	3

The normal operation sample data acquired by sensors in the RCS are used to train the PCA model. Further, the PCA-based fault detection module is running online (Lu 2005) and T^2 statistics, SPE statistics and the relevant limits are observed synchronously, as shown in Fig. 6.

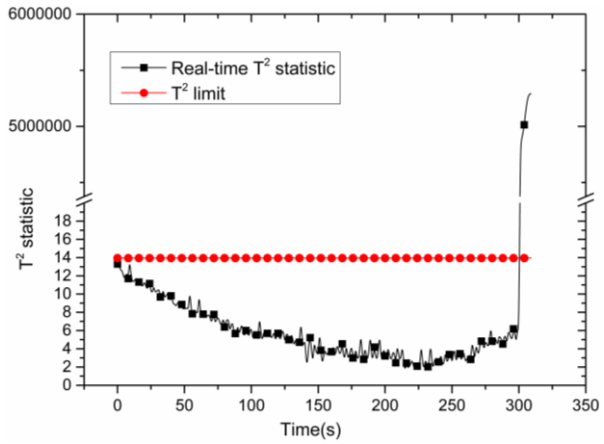

Fig. 6(a) Change in trends of T^2 statistics.

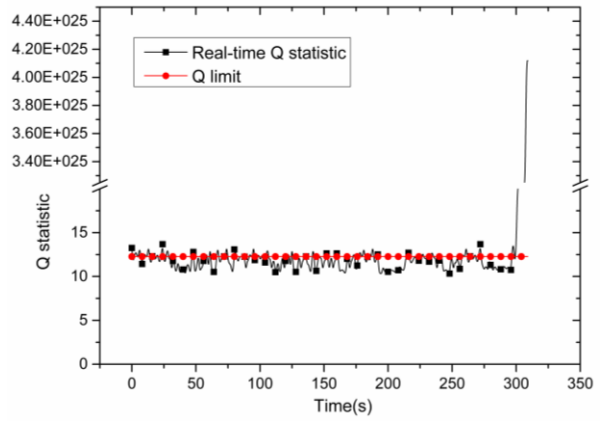

Fig. 6(b) Change in trends of Q statistics.

As observed during the normal operation of NPP, T2 statistics and Q statistics exceed their limits sometimes. But according to the binomial probability distribution proposed in this paper, these alarms are false alarms, so the on-line monitoring continues. Then in 301s, T2 statistics and Q statistics exceed their limits. Moreover, after 303s, the abnormality could be confirmed because the allowable number of false alarm is 3. Hence, there is a malfunction in the RCS but we cannot locate where the fault is yet. That is, the operators cannot rely on the results to analyze the root causes of the alarms. On this basis, the fault type and location are analyzed further.

3.3 Evaluation of the on-line fault type diagnosis

The proposed methodology is able to utilize historical failure data for training and learning. However, such data are limited. Thus, a number of training data under various fault conditions can be derived by utilizing the existing simulation model. While the NPP model is in normal operating condition, the simulation model runs, mimicking the real-time operation of the NPP. After abnormality has been detected by PCA model, the simulation model is transferred to off-line status so that different failure mode can be provided for AIA model for its fault diagnosis. After checking the positions of valves and pumps in RCS to eliminate some general malfunctions, five common failure modes with similar changes in trends in some parameters are selected. The simulation model uses these failure modes to do its calculations, 5 times faster-than-real-time, and the calculated values serves to provide training data according to the changes in parameters as shown in Fig. 5. Since the malfunctions in 2# loop are similar with 1# loop, this paper only utilizes malfunctions in 1# loop to test the effectiveness of AIA. These five failure modes are leakage in 1# cold leg pipeline, leakage in 1# hot leg pipeline, steam generator tube rupture (SGTR) in 1# loop and false injection of safety injection system (FSIS). By comparing the changes in the trends of these parameters with safety analysis report, we observed that the fault degree is not severe. Hence, these small degree malfunctions is simulated at random. Finally, the trends of 26 measured parameters are acquired, as shown in Table 1. Also, Fig.7 shows the pressure of pressurizer under different failure modes.

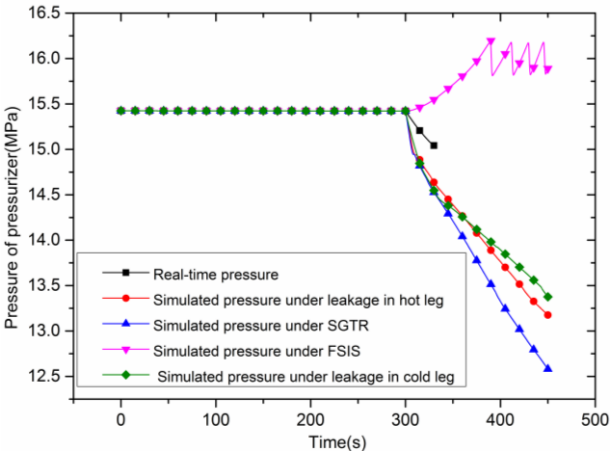

Fig. 7 Change trends under different failure modes.

After normalization and standardization of these data $X_1 = (x_{i1}, x_{i2}, ..., x_{i26})$, $X_2 = (x_{i1}, x_{i2}, ..., x_{i26})$ …, $X_4 = (x_{i1}, x_{i2}, ..., x_{i26})$, where x_1, x_2, x_3, x_4,…, x_{26} are connected with parameters in Table 1.

Moreover, real-time data and failure data are folded for every time step to get the 4×7 data matrix. And then, singular decomposition is implemented for each data matrix to obtain all the singular values in each situation. Table 3 shows the singular values in 100s after the fault occurs.

Table 3 Singular values under different failure modes

No.	Category	Singular value 1	Singular value 2	Singular value 3	Singular value 4
1	Leakage in hot leg	1.2170	0.4270	0.0828	0.0098
2	SGTR	1.3668	0.5306	0.1724	0.1062
3	FSIS	0.6107	0.1208	0.0499	0.0157
4	Leakage in cold leg	1.0318	0.3870	0.0098	0.0045

And then, according to the following relation

$$(\theta_1+\theta_2+\ldots+\theta_k)/\sum_1^n\theta_i \geq 90\%$$

the simplified singular values are selected. Hence, the antigen and antibody for each failure mode for every second are displayed as shown in Table 4.

Table 4 Antigens and antibodies under different failure modes

No.	Category	Antigen	Antibody
1	Leakage in hot leg	(-0.9119,-0.2810,-0.2700,-0.1288)	(-0.274,-0.159,-0.166,0.156,-0.158,-0.194,-0.886)
		(0.3720,-0.4467,-0.4768,-0.6594)	(-0.555,-0.333,-0.312,-0.319,-0.309,-0.272,0.460)
2	SGTR	(-0.7814,-0.4244,-0.3770,-0.2591)	(-0.453,-0.194,-0.157,-0.232,-0.219,-0.382,-0.696)
		(0.5483,-0.3232,-0.2783,-0.7193)	(-0.504,-0.290,-0.191,-0.347,-0.363,0.190,-0.578)
		(0.2869,-0.6789,-0.2594,0.6241)	(-0.032,0.106,-0.017,-0.646,0.491,0.525,-0.232)
3	FSIS	(-0.5139,-0.5343,-0.5197,-0.4370)	(-0.497,-0.391,-0.344,-0.330,-0.330,-0.379,-0.347)
		(0.0402,-0.4496,-0.2946,0.8423)	(0.131,0.294,0.095,0.113,0.114,0.090,-0.924)
4	Leakage in cold leg	(-0.8474,-0.3600,-0.3443,-0.1835)	(-0.410,-0.157,-0.152,-0.151,-0.153,-0.360,-0.780)
		(0.4672,-0.3505,-0.4099,-0.7006)	(-0.690,-0.248,-0.255,-0.262,-0.231,0.092,0.517)

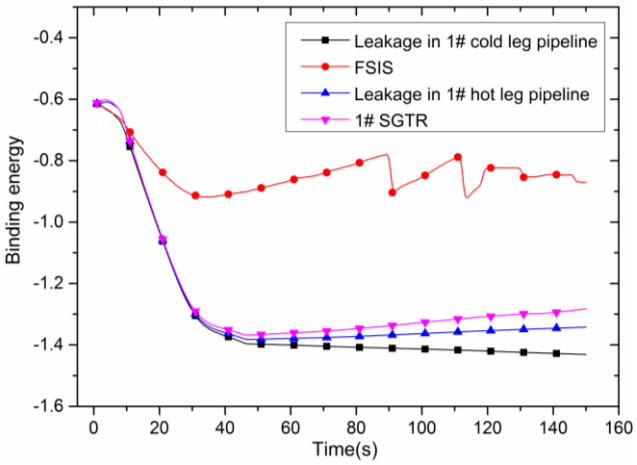

Fig. 8 Real-time binding energy in AIA.

Finally, the binding energy of measured data and every simulated data after malfunction occurs are displayed in Fig.8. It can be seen that the binding energy of leakage in 1# cold leg pipeline is the lowest 40-50 seconds later after the fault occurs.

3.4 Verification and comparison of on-line failure degree assessment

After detecting and diagnosing the fault as a leakage in 1# cold leg pipeline, the specific degree of this fault is assessed by combining PCA model with distance functions. At first, the off-line simulation model is reset to the scenario where the abnormality is detected by PCA-based on-line monitoring. Meanwhile, according to the safety analysis reports of NPP, the pressure and water level in the secondary loop of the SG changes distinctly when the leakage in the pipeline is more than $10cm^2$. However, it does not occur in this case.

Hence, the leakage area must be less than $10cm^2$. After that, leakages with the magnitude of $8cm^2$, $6cm^2$, $4cm^2$, $2cm^2$ and 1 cm^2 respectively are injected into the 1# cold leg coolant pipe in the simulation model to get the training data for failure degree assessment. Figure 9 shows the values of some measured and the corresponding simulated parameters in different failure degree.

Besides, 26 measured and simulated data in different failure degree are normalized together. After that, PCA model discussed in section 2.2 is adopted for reducing the dimension of the data. Thus, the selected PCs and the corresponding eigenvector reconstitute

the estimated vectors. As shown in Table 5, 100s after the failure is detected; the dimensions of the estimated vectors are reduced from 26 to 6.

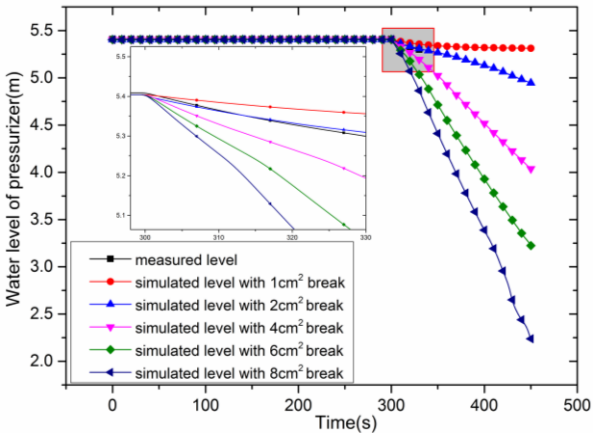

Fig. 9(a) Water level of pressurizer in different failure magnitude.

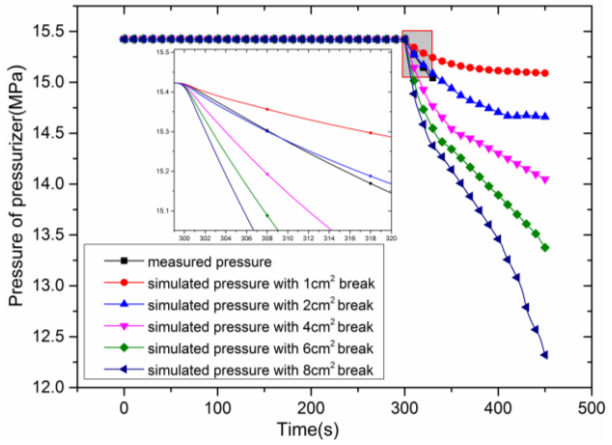

Fig. 9(b) Pressure of pressurizer in different failure magnitude.

Table 5 status estimate vectors of original vectors

No	Name	Estimate vector
1	Measured values	(-1.0164,0.1977,-0.0359,-0.0372,-0.0075,-0.0070)
2	Simulated values with 1cm² break	(-0.6794,0.2103,-0.0141,-0.000323,0.0179,0.0086)
3	Simulated values with 2cm² break	(-1.0217,0.1928,-0.0496,0.0155,-0.0082,0.0131)
4	Simulated values with 4cm² break	(-1.1222,-0.0221,-0.0771,-0.004,0.0047,0.0088)
5	Simulated values with 6cm² break	(-1.2199,-0.2298,-0.1092,-0.0237,0.0123,0.0114)
6	Simulated values with 8cm² break	(-1.3174,-0.4345,-0.1482,-0.0362,0.0098,0.0195)

Furthermore, these vectors are mapped as points and then calculated by Euclidean distance model and Mahalanobis distance model. Figure 10 shows the Euclidean distance curves with real-time data and simulated values under different failure degree. The base-10 logarithm of Mahalanobis distance curves is presented in Fig.11.

100s later after abnormality detection, these distance curves are integrated with the event time respectively. The results show that the integral curves of Euclidean distance under 2cm^2 leakages are similar with real-time data, and relative error is 1.10%. Moreover, the integral curves of Mahalanobis distance under 2cm^2 leakages are also similar with real-time data, and relative error is 1.33%. This result shows that the Mahalabonis distance and Euclidean distance are effective for failure degree assessment. It also shows that the combination of Euclidean distance and PCA model are much better, as the Mahalabonis distance represents the covariance distance of the sample and the inputs for Mahalabonis distance do not need to be normalized. However, the inputs for PCA model must be normalized, which invariably shadows the advantages of Mahalabonis distance. On the contrary, Euclidean distance shows the absolute distance of the estimated vectors which is in a lower dimension. In other word, PCA model and Euclidean distance make up for each other. As a result, the entire failure information is that there is leakage in 1# cold leg coolant pipeline and the leakage area is 2cm^2. Consequently, these messages will be displayed in HMI to warn the operators concerning the severity of current malfunction.

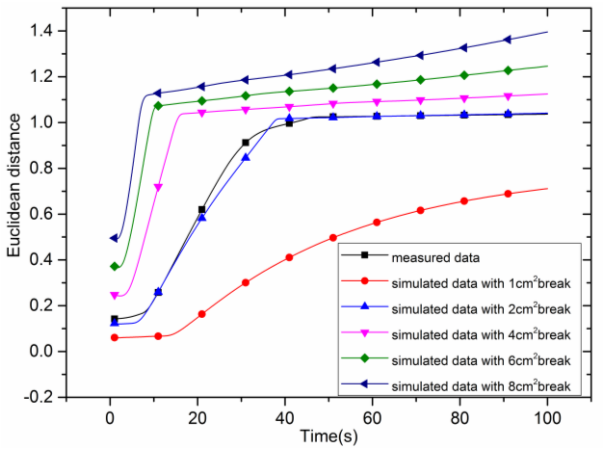

Fig.10. Euclidean distance after simplified by PCA.

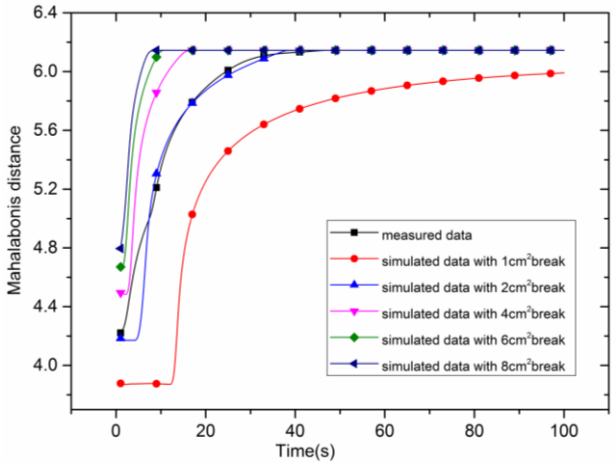

Fig.11 Mahalabonis distance after simplified by PCA.

4 Conclusions

An integrated methodology for online fault detection, diagnosis and failure degree assessment is proposed in this paper based on optimized PCA, AIA and similarity measurement. It is a novel, enhanced data-driven diagnostic method and is much suitable to solve problems related to on-line fault diagnosis for complex systems such as NPP. Detailed mechanism analysis is described to be of positive significance in preparing for model construction and it proves that we can achieve better diagnostic accuracy. Utilizing thermal-hydraulic simulation model to provide on-line sample data, a case analysis is used to verify the accuracy and effectiveness of this methodology, and the approach shows the following merits:

(1) The improved PCA-based abnormal detection is used to detect the malfunctions on time and it reduced the occurrence of false alarms to the minimum.

(2) AIA-based fault type diagnosis with capability for on-line training is proposed and implemented on real-time data, resulting in a better pattern recognition.

(3) Failure degree assessment is achieved by utilizing PCA and two typical distance functions – the Euclidean distance and the Mahalanobis distance - to lower the dimension of parameters, and for similarity measurement respectively. In addition, these distance functions are compared to select the best alternative.

In conclusion, this improved data-driven methodology utilized for fault detection and diagnosis is feasible and practical. More importantly, this methodology - which is a part of computerized operator support system - can be extended to diagnose faults in other components of PWR, other types of NPP or even on other complex thermal plants, to maintain the safety and reliability. Further, it also presents good foundation to enhance the research depth in the study of on-line risk monitoring systems.

Acknowledgement

This work is funded by Chinese national research project “Research of Online Monitoring and Operator Support Technology”.

References

[1] THOMAS, U., and ROGER, L., *et al.*: A computerized operator support system prototype [R]. INL/EXT-15-36788. 2015: Idaho National Laboratory.

[2] IAEA: Diagnostic and prognostic techniques in monitoring structures, systems and components in nuclear power plants [R]. 2013: No.NP-T-3.14.

[3] KIM, H., MAN, G.N., and HEO, G.: Application of monitoring, diagnosis, and prognosis in thermal performance analysis for nuclear power plants [J]. Nuclear Engineering & Technology, 2014, 46(6): 737-752.

[4] SOON, H.C., KI, S.K., and SEONG, S.C., *et al.*: Development of the on-line operator aid system OASYS using a rule-based expert system and fuzzy logic for nuclear power plants [J]. Reactor Control, 1995, 112:266-294.

[5] HINES, J.W., GARVEY, D., and SEIBERT, R.: Process and equipment monitoring methodologies applied to sensor calibration monitoring [J]. Quality and Reliability Engineering International, 2007, 23(1): 123-135.

[6] CILLIERS, A.C.: Correlating hardware fault detection information from distributed control systems to isolate and diagnose a fault in pressurized water reactors [J]. Annals of Nuclear Energy, 2013, 54: 91-103.

[7] LI, P.C., and CHEN, G.H., *et al.*: Methodology for analyzing the dependencies between human operators in digital control systems [J]. Fuzzy Sets and Systems, 2016, 293: 127-143.

[8] LIU, P., and LI, Z.Z.: Comparison between conventional and digital nuclear power plant main control room: A task complexity perspective, part I: Overall results and analysis [J]. International Journal of Industrial Ergonomics, 2016, 51:2-9.

[9] LIND, M.: An introduction to multilevel flow modeling [J]. Journal of Nuclear Safety and Simulation, 2011, 2(1): 22-32.

[10] BJORLO, T.J., and BERG, O.: Use of Computer-Based Operator Support Systems in Control Room Upgrades and New Control Room Designs for Nuclear Power Plants [J]. Proceedings NPIC&HMIT '96, 1996: P1397-1404.

[11] JAQUES, R., and THOMAS, W.: PRODIAG: A Process-Independent Transient Diagnostic System-II: Validation Tests [J]. Nuclear Science and Engineering: Elsevier, 1999, 131(3):348-369P.

[12] KAMAL, H., MEISAM, P., and HOSEIN, M.: Fault diagnosis and classification based on wavelet transform and neural network [J]. Progress in Nuclear Energy, 2011, 53(6):41-47.

[13] HINES, J.W., and DAVIS, E.: Lessons learned from the U.S. nuclear power plant on-line monitoring programs [J]. Progress in Nuclear Energy, 2005, 46(3-4): 176-189.

[14] ZIO, E., and GOLA, G.: Neuro-fuzzy pattern classification for fault diagnosis in nuclear components [J]. Annals of Nuclear Energy, 2006, 33:415-426.

[15] WOLBRECHT, E., AMBROSIO, B.D., and PASSCH, B.: Monitoring and diagnosis of a multi-stage manufacturing process using bayesian networks [J]. Artificial Intelligence for Engineering, Design and Manufacturing, 2000, 14(2):53-67.

[16] ISHIGURO, A., WATANABE, Y., and UCHIKAWA, Y.: Fault diagnosis of plant systems using immune networks. Proc IEEE International Conference on Multi-Sensor Fusion Integration for Intelligent Systems [J]. Las Vegas, NV, 1994: 34-42.

[17] WANG, H., and PENG, M.J., *et al.*: Improved methods of online monitoring and prediction in condensate and feed water system of nuclear power plant [J]. Annals of Nuclear Energy, 2016, 90(4): 44-53.

[18] DANESHVAR, M., and FARHANGI, B.: Data driven approach for fault detection and diagnosis of boiler system in coal fired power plant using principal component analysis [J]. International Review of Automatic Control (IREACO), 2010, 3(2): 198-208.

[19] LU, B., and UPADHYAYA, B.R.: Monitoring and fault diagnosis of the steam generator system of a nuclear power plant using data-driven modeling and residual space analysis [J]. Annals of Nuclear Energy, 2005, 32(9): 897-912.

[20] ZHANG, B.D., ZHOU, A.H., CUI, X.M., and DONG, P.: The research of immune system for the diagnosis of steam turbine generator unit. Turbine Technology. 2007, 49: 376-378 (in Chinese).

[21] ISHIDA, Y.: An Immune Network Approach to Sensor-Based Diagnosis by Self-Organization. Complex Systems. 1996, 10, 73-90.

[22] ZHANG, H.L., LIU, S.L., JIAO, W.H., and LI, D.: The machine abnormal degree detection method based on SVDD and negative selection mechanism. Journal of Vibro-engineering. 2013, 15 (4), 1873-1884.

[23] TARAKANOV, A., and DASGUPTA, D.A.: A formal model of artificial immune system. Biosystems. 2000, 55(1-3), 151-158.

[24] LI, X., DEZERT, J., and SMARANDACHE, F., *et al*.: Evidence supporting measure of similarity for reducing the complexity in information fusion [J]. Information Sciences, 2011, 181(4):1818-1835.

[25] PARK, S., PARK, J., and HEO, G.: Transient diagnosis and prognosis for secondary system in nuclear power plants [J]. Nuclear Engineering and Technology, 2016, 48(5): 1184-1191.

[26] QIN, S., and RICARDO, D.: Determining the number of principal components for best reconstruction [J]. Journal of Process Control, 2000, 10(2): 245-250.